Neuropsychopharmacology

ARTICLE

Longitudinal imaging of metabotropic glutamate 5 receptors during early and extended alcohol abstinence

Ansel T. Hillmer[1,2,3,4], Gustavo A. Angarita[1,5], Irina Esterlis[1,3], Jon Mikael Anderson[1], Nabeel Nabulsi[2,3], Keunpoong Lim[2,3], Jim Ropchan[2,3], Richard E. Carson[2,3,4], John H. Krystal[1], Stephanie S. O' Malley[1] and Kelly P. Cosgrove[1,2,3]

Chronic alcohol use has important effects on the glutamate system. The metabotropic glutamate 5 (mGlu5) receptor has shown promise in preclinical models as a target to reduce drinking-related behaviors and cue-induced reinstatement, motivating human studies of mGlu5 receptor negative allosteric modulators. The goal of this work was to measure levels of mGlu5 receptor availability with positron emission tomography (PET) imaging using the mGlu5 receptor-specific radiotracer [^{18}F]FPEB during early and extended alcohol abstinence. Subjects who met DSM-5 criteria for alcohol use disorder (AUD; $n = 17$) were admitted inpatient for the study duration. [^{18}F]FPEB PET scans were acquired first during early abstinence (6 ± 4 days after last drink) and a second time during extended abstinence ($n = 13$; 27 ± 6 days after last drink). A single scan was acquired in healthy controls matched for sex and smoking status ($n = 20$). [^{18}F]FPEB total volumes of distribution (V_T) corrected for partial volume effects were measured using equilibrium analysis throughout the brain. A linear mixed model controlling for smoking status and sex identified significantly higher [^{18}F]FPEB V_T in AUD subjects at early abstinence compared to controls ($F_{(1,32)} = 7.23$, $p = 0.011$). Post-hoc analyses revealed this effect to occur in cortical brain regions. No evidence for significant changes in [^{18}F]FPEB V_T over time were established. These findings provide human evidence consistent with a robust preclinical literature supporting mGlu5 receptor drugs as pharmacotherapies for AUD.

Neuropsychopharmacology (2021) 46:380–385; https://doi.org/10.1038/s41386-020-00856-9

INTRODUCTION

Alcohol use disorder (AUD), which affects over 10% of the population, alters neurotransmitter function [1, 2] and neural organization [3]. During alcohol abstinence, the brain again undergoes dynamic changes that have important implications for treatment outcome [4]. Glutamate is a key neurotransmitter influenced by chronic alcohol use [5], evidenced by upregulation of the key receptor *N*-methyl-D-aspartate (NMDA) [6] and excessive excitatory signaling and glutamate levels during withdrawal [7]. These aggregate changes increase relapse propensity [8], making the glutamatergic system of high interest to promote recovery during abstinence.

The metabotropic glutamate 5 (mGlu5) receptor has shown promise as a drug development target for improving alcohol-related outcomes. MGlu5 receptors are primarily postsynaptic G-protein coupled receptors intracellularly coupled to NMDA receptors by the scaffolding proteins Homer and Shank [9–11], thereby modulating NMDA function. In preclinical models, negative allosteric modulation, antagonism, or deletion of mGlu5 receptors reduced alcohol self-administration [12–15] and diminished reinstatement [16–18]. In humans, genetic variations in *MGLUR5* are associated with AUD [19]. Indeed, mGlu5 receptor negative allosteric modulation is a particularly attractive mechanism for AUD that has motivated human laboratory studies evaluating safety and tolerability [20] and alcohol effects on pharmacokinetics [21] of a negative allosteric modulator.

Measurements of mGlu5 receptor levels in humans might further implicate this target in the pathophysiology of human AUD. In post mortem brain tissue, mGlu1/5 receptor binding was greater in the AUD brain compared to controls [22, 23]. In vivo positron emission tomography (PET) imaging with radioligands specific for mGlu5 receptor revealed mixed findings. One study using the radioligand [^{11}C]ABP688 involving 14 nonsmoking men with AUD reported higher mGlu5 receptor availability in temporal lobe compared to controls [24]. A larger study using the radioligand [^{18}F]FPEB in men and women with AUD, but without controlling for tobacco smoking, reported lower mGlu5 receptor availability in limbic brain regions compared to controls [25], which recovered after 6 months abstinence [26]. Since multiple reports identify lower mGlu5 receptor availability in tobacco smokers [27, 28], we hypothesized that when controlled for smoking mGlu5 receptor availability would be higher in AUD, consistent with post-mortem and preclinical data. Thus, the goal of this work was to assess mGlu5 receptor levels using the PET radiotracer [^{18}F]FPEB [29] in people with AUD at multiple longitudinal timepoints in an independent sample featuring a control group matched for sex and tobacco smoking status.

[1]Department of Psychiatry, Yale University School of Medicine, New Haven, CT, USA; [2]Department of Radiology and Biomedical Imaging, Yale University School of Medicine, New Haven, CT, USA; [3]Yale PET Center, Yale University School of Medicine, New Haven, CT, USA; [4]Department of Biomedical Engineering, Yale University, New Haven, CT, USA and [5]Clinical Neuroscience Research Unit, Connecticut Mental Health Center, New Haven, CT, USA
Correspondence: Ansel T. Hillmer (ansel.hillmer@yale.edu)

Received: 27 May 2020 Revised: 10 August 2020 Accepted: 27 August 2020
Published online: 12 September 2020

METHODS

Participants

Study participants included 17 subjects with AUD (4 women, 13 men) and 20 healthy control subjects (7 women, 13 men) recruited from the local population. All procedures were approved by the Yale School of Medicine Human Investigation Committee and the Radiation Safety Committee. Written informed consent was obtained from all subjects prior to participation in this study.

Participants with AUD met DSM-5 criteria for AUD. During screening or inpatient admission, the SCID-5 identified secondary comorbid diagnoses for five subjects (two PTSD, two major depressive disorder, one generalized anxiety disorder) of whom two were on active medication (both for major depressive disorder, one on fluoxetine, one on trazadone and sertraline). Participants with AUD were admitted to the Connecticut Mental Health Center Clinical Neuroscience Research Unit and remained on the unit until scanning procedures were completed. While on the unit, alcohol withdrawal symptoms were assessed daily with the Clinical Institute Withdrawal Assessment for Alcohol-revised (CIWA-R) [30]. Of the 17 AUD participants, 7 underwent detoxification without medication, while 10 underwent medicated detoxification with lorazepam (mean cumulative dose, 11 ± 7 mg, range 2–19 mg) over no more than 5 days since last drink (average 3 days) to alleviate withdrawal symptoms. Lorazepam was administered on the day of first scan for two subjects. Prior to admission, alcohol use over the prior 90 days was evaluated with the timeline-follow back interview [31].

A first [^{18}F]FPEB PET scan was acquired during early abstinence 6 ± 4 days after last drink (range, 2–14 days). Of the 17 AUD participants, 13 participated in a second [^{18}F]FPEB PET scan that occurred 20 ± 5 days after the initial scanning session and 27 ± 6 days after the last drink (range, 17–36 days after the last drink). On PET scan days, craving for alcohol was evaluated with the Alcohol Craving Questionnaire [30]. Each PET imaging scan was accompanied by a corresponding MRI scan that occurred within 3 days.

Healthy controls had no history of significant major medical disorders and did not meet criteria for current or past psychiatric or substance use diagnosis (other than nicotine use) as confirmed by the SCID-5. Control subjects reported drinking <6 alcohol drinks per week. These subjects participated in a single [^{18}F]FPEB scan. Participant demographics and PET imaging parameters are summarized in Table 1.

Table 1. Participant Demographics and Scanning Parameters.

	Alcohol use disorder group		Healthy control group
	Scan 1 (n = 17)	Scan 2 (n = 13)	(n = 20)
Sex	4F/13M	3F/10M	7F/13M
Age (year)	42.3 ± 8.7	43.2 ± 8.5	39.6 ± 12.7
Tobacco smokers	n = 12	n = 10	n = 7
Years AUD	26 ± 7	27 ± 7	
Drinks per week (TLFB)	77 ± 42	84 ± 40	
Drinks per drinking day (TLFB)	12 ± 7	13 ± 8	
Days abstinence	6 ± 4	27 ± 6	
Peak alcohol withdrawal (CIWA-R)	3 ± 3 (range, 0–10)	3 ± 3 (range, 0–10)	
Alcohol craving (ACQ)	120 ± 35	92 ± 60	
Injected dose (MBq)	157.6 ± 43.3	149.8 ± 45.7	170.7 ± 12.0
Injected mass (μg)	0.32 ± 0.19	0.29 ± 0.17	0.39 ± 0.20

Summary of participant demographics, clinical measures, and scanning parameters. Values are mean ± standard deviations.
TLFB timeline follow back (on admittance day), *CIWA-R* Clinical Institute Withdrawal Assessment for Alcohol-revised, *ACQ* alcohol craving questionnaire.

Scan data acquisition

[^{18}F]FPEB was produced via nucleophilic substitution of ^{18}F-fluoride with the *nitro-* precursor as detailed previously [32], resulting in high molar activities of 136 ± 62 MBq/nmol. PET-imaging data were acquired with a high-resolution research tomograph (HRRT; Siemens). Head motion data were simultaneously acquired with an optical motion-tracking tool (Vicra, NDI Systems). A total of 171 ± 12 MBq [^{18}F]FPEB was administered as a bolus plus constant infusion with K_{bol} = 190 min [33], targeting equilibrium conditions between arterial plasma, venous plasma, and tissue concentrations within 90 min. Therefore, emission data acquisition began 90 min after [^{18}F]FPEB was first administered, and continued for 30 min. A ^{137}Cs transmission was also acquired for 6 min for attenuation correction. Venous plasma samples were acquired at discrete time points from 60 to 120 min. At minimum, five venous plasma samples were acquired during the 90–120 min equilibrium period, of which no less than 3 were included for metabolite analyses. The metabolite-corrected venous input function, which provides excellent concordance with the arterial input function after 60 min [^{18}F]FPEB infusion [34], was measured as previously described [33]. All scanning procedures occurred within a 3 h period in the early afternoon to minimize the effects of within-day variation in mGlu5 receptor availability [35].

Magnetic resonance image (MRI) data were acquired for anatomical localization of [^{18}F]FPEB uptake. MR data were acquired with a 3 T Trio Scanner (Siemens Medical Systems, Erlangen, Germany) with a weighted gradient-echo (MPRAGE) sequence featuring the following parameters: (TE = 3.3 ms; TI = 1100 ms, TF = 2500 ms, FA = 7°) yielding 1 mm^3 isotropic resolution.

Image processing and analysis. Dynamic list-mode PET data were histogrammed into discrete time frames up to 5 min and reconstructed with the MOLAR algorithm [36]. To transform PET data into MR space, a summed image of the first 10 min of PET data was registered to the subject-specific T1-weighted MRI using a mutual information algorithm with six degrees of freedom (FLIRT, FSL 3.2; Analysis Group; FMRIB, Oxford, UK). The native MRI was segmented with the Computational Anatomy Toolbox (CAT12; https://www.neuro.uni-jena.de) and co-registered to the Montreal Neurological Institute (MNI) template space with a nonlinear transformation algorithm (BioImage Suite; https://www.bioimagesuite.com) for Region of Interest (ROI) definition. The dynamic PET data were corrected for partial volume effects using CAT12 segmentations with previously published methods [37]. The time–activity curves of radioactivity concentration in tissue were extracted using the Automated Anatomical Labeling atlas [38] from the following bilateral brain regions: dorsolateral prefrontal cortex (dlPFC), orbitofrontal cortex (OFC), ventromedial prefrontal cortex (vmPFC), cingulate gyrus, insula cortex, parietal cortex, temporal cortex, occipital cortex, cerebellum, thalamus, caudate, putamen, amygdala, hippocampus.

The primary outcome measure of [^{18}F]FPEB data was the total volume of distribution (V_T), which is the equilibrium ratio of [^{18}F]FPEB concentration in tissue to that in venous plasma [39]. This outcome measure was selected because significant specific mGlu5 receptor binding is found throughout the human brain [40], meaning reference region approaches could be biased by individual variation in specific radiotracer uptake. [^{18}F]FPEB V_T is proportional to the number of mGlu5 sites available for [^{18}F]FPEB binding. Equilibrium analysis was used to estimate [^{18}F]FPEB V_T.

However, non-equilibrium conditions were observed for a number of subjects. This could occur due to altered metabolic conversion of [^{18}F]FPEB in these subjects, a phenomenon previously reported for a similar mGlu5 receptor ligand in the presence of alcohol [21]. To correct for non-equilibrium conditions a tissue clearance correction was applied to all regional V_T equilibrium estimates in all subjects using the [^{18}F]FPEB-specific value of $\gamma = 4.3$ min cm^3/mL [41]. This correction significantly reduced variance in both study groups (Morgan–Pitman test), consistent with the initial validation results [41].

Statistical analysis

[^{18}F]FPEB V_T values were analyzed with a linear mixed modeling approach. To test the null hypothesis of no difference in [^{18}F]FPEB V_T between healthy controls and the AUD group at ~1 week of abstinence, a model was constructed with diagnosis as a between-subjects factor and region as a within-subjects factor. Based on previously reported results, additional factors accounting for subject age, smoking status [27, 28], and subject sex [42, 43] were considered in the model, with the best-fitting structure selected based on the Bayes–Schwartz information criterion. To test the null hypothesis of no change in [^{18}F]FPEB V_T over time in the AUD group, a model with region and time as within subjects factors including subject smoking status and age was constructed. Main effects were considered significant for $\alpha < 0.05$. Post-hoc linear contrasts examined regional differences in [^{18}F]FPEB V_T between AUD subjects and healthy controls controlling for the statistically significant factors identified from the above analysis. To visually assess brain areas of particularly large group differences in mGlu5 receptor availability, exploratory voxelwise analyses were performed with PVC-corrected V_T images smoothed with an 8 mm Gaussian kernel in SPM12. For consistency with ROI-level results, group differences between healthy controls and AUD at ~1 week abstinence were assessed with a full factorial design including AUD diagnosis and smoking as main factors. The longitudinal images were conducted as a paired *t*-test including smoking status as a covariate. Statistical thresholds were set at $p < 0.05$, familywise error corrected.

Exploratory analyses were conducted to examine relationships between regional mGlu5 receptor availability and clinical measures within the AUD group. Due to the exploratory nature, these were uncorrected for multiple comparisons. Regression analysis examined relationships of regional [^{18}F]FPEB V_T during early abstinence with average drinks per week, time of last drink, time of last benzodiazepine administration, peak CIWA-R score, and craving on scan day. A second set of regression analyses examined relationships between the change in [^{18}F]FPEB V_T with the duration of abstinence, amount of drinking, or peak CIWA-R score. Finally, repeated measures correlations between alcohol craving on scan day and regional [^{18}F]FPEB V_T were calculated to examine within-individual relationships between these variables. All statistical analyses were conducted with R (version 3.5.1).

RESULTS

A model including main factors of sex and smoking status with AUD diagnosis and region best described the data comparing AUD subjects at early abstinence with healthy controls. A significant main effect of AUD diagnosis was observed ($F_{(1,32)} = 7.23$, $p = 0.011$) in addition to a trend for a main effect of smoking ($F_{(1,32)} = 3.78$, $p = 0.06$) but not sex ($F_{(1,32)} = 1.68$, $p = 0.20$). Post-hoc linear contrasts revealed significantly higher (uncorrected for multiple comparisons) mGlu5 receptor availability for AUD diagnosis in the dlPFC, OFC, occipital cortex, and temporal cortex, with a trend in the vmPFC and parietal cortex. These findings are shown in Fig. 1. Exploratory voxelwise analyses did not provide further insight into group differences in [^{18}F]FPEB V_T.

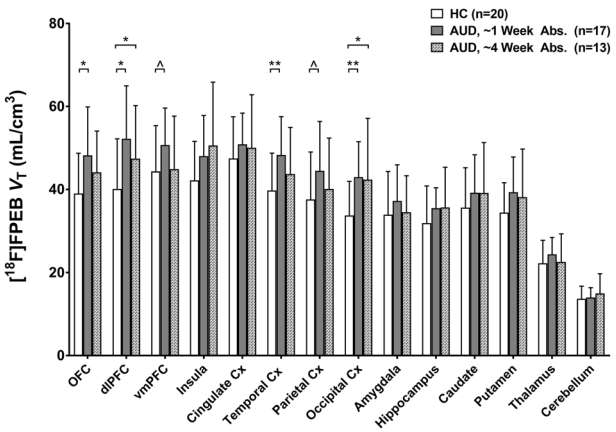

Fig. 1 MGlu5 receptor availability in AUD. [^{18}F]FPEB total distribution volume (V_T), a measure of mGlu5 receptor availability, in AUD at ~1 week abstinence (solid dark bars), ~4 weeks abstinence (patterned dark bars) and healthy controls (open bars). [^{18}F]FPEB V_T values include partial volume correction. *Abbreviations*: OFC orbitofrontal cortex, dlPFC dorsolateral prefrontal cortex, vmPFC ventromedial prefrontal cortex. Main effects for post-hoc analyses are denoted as: $^{**}p < 0.01$; $^{*}p < 0.05$; $^{\wedge}p < 0.10$. Error bars indicate standard deviations.

The longitudinal data were best described by a model including main factors of smoking status and time. The model did not establish evidence for a within-subjects change in [^{18}F]FPEB V_T during abstinence ($F_{(1,21)} = 2.83$, $p = 0.11$). A secondary analysis comparing [^{18}F]FPEB V_T in AUD at extended abstinence with healthy controls revealed no statistically significant between-group differences ($F_{(1,28)} = 2.95$, $p = 0.10$), while the effect of smoking was significant ($F_{(1,28)} = 11.2$, $p = 0.002$) with significantly lower [^{18}F]FPEB V_T in smokers compared to nonsmokers. These data are illustrated in Fig. 1. Exploratory voxelwise analysis did not identify clusters of [^{18}F]FPEB V_T that changed over time.

Within the AUD group, secondary analyses revealed no significant relationships of mGlu5 receptor availability at early abstinence with the amount of drinking, time of last drink, time of last benzodiazepine administration, or peak CIWA-R score. A trend for greater alcohol craving on scan day corresponding to greater mGlu5 receptor availability in vmPFC during early abstinence was identified ($F_{(1,15)} = 3.75$, $p = 0.07$ uncorrected). No evidence was observed for relationships of change in mGlu5 receptor availability with duration of abstinence, amount of drinking, of peak CIWA-R score, or change in craving. No evidence was observed for relationships of changes in craving and changes in mGlu5 receptor availability within subjects.

DISCUSSION

Our data indicate higher mGlu5 receptor availability in cortical brain regions in subjects with AUD at early (~1 week) abstinence compared to healthy controls that did not significantly change when measured a second time following extended (~4 weeks) abstinence. This result extends previous reports of higher mGlu5 receptor binding in AUD post mortem brain [23] and higher mGlu5 receptor availability in individuals with AUD conducted after 25 days of abstinence [24]. In the context of a robust preclinical literature identifying mGlu5 receptor inhibition as a mechanism that reduces alcohol drinking and reinstatement, these aggregate findings provide in vivo human evidence consistent with continued pursuit of therapeutics that modulate mGlu5 receptor signaling for the treatment of AUD.

The within-subject longitudinal design across abstinence represents a strength of this study. Specifically, given glutamatergic fluctuations that occur during early alcohol abstinence [44],

the inclusion of an early abstinence timepoint provides important data regarding mGlu5 receptor dynamics during abstinence, where levels are clearly higher than control levels. The data acquired during extended abstinence are not conclusive regarding mGlu5 receptor 'normalization' or consistently higher availability, as neither main effects of time within the AUD subjects nor the diagnostic group comparison of AUD at extended abstinence with controls were significant. To provide some preliminary insight into this question, exploratory analyses at the regional level investigated for within-subject changes of [^{18}F]FPEB V_T over time, and compared control values with those measured in AUD at extended abstinence (uncorrected for multiple comparisons). This exploratory analysis did not identify any within-subject regional differences in [^{18}F]FPEB V_T, while some evidence for higher [^{18}F]FPEB V_T in AUD at extended abstinence in the dlPFC and occipital cortex was found. Given the exploratory nature of this analysis, these differences are highly preliminary and require a larger sample for conclusive results. Since other brain measures such as gray matter volume require over 2 months to recover in AUD [45], potential 'normalization' effects may occur at timescales beyond the scope of this study. Thus, the presented data do not clarify whether mGlu5 receptor availability is a consequence of chronic alcohol use or withdrawal, or exists prior to AUD onset. However, preclinical data demonstrate dynamic changes in mGlu5 levels following drug administration, including alcohol [46, 47], which seem to be complex depending on duration of drug administration and time of withdrawal [48]. This literature suggests that the observed higher mGlu5 receptor availability may result from chronic alcohol use and abstinence, but further research in this area is needed.

The presented study included tobacco smokers in both AUD and control groups, which is a critical consideration since smoking rates are considerably higher in people with AUD compared to the general population [49]. Furthermore, multiple studies report lower mGlu5 receptor availability in tobacco smokers compared to nonsmokers [27, 28]. Consistent with these reports, in the presented data mGlu5 receptor availability was lower in tobacco smokers regardless of AUD status, as illustrated in Supplementary Fig. 1. This result may explain discrepant reports of lower mGlu5 receptor availability (vs. higher mGlu5 receptor availability in the current study) in people with AUD compared to controls [25, 26], as these previous studies included smokers in the AUD group but not the control group. Although the data from this study show no evidence for interactions of smoking with either AUD diagnosis or over time within AUD subjects, the sample size was not well powered to examine fully these effects. Further work is required to confirm this initial result.

Secondary analyses revealed a trend for higher mGlu5 receptor availability in vmPFC with greater craving for alcohol during early abstinence (see Supplementary Fig. 2). While this trend was not statistically significant and there was no evidence for this relationship within individuals over time, it notably complements previous PET imaging reports of the same relationship [25]. Moreover, these results, albeit preliminary, provide human data consistent with an extensive preclinical literature in support of mGlu5 receptor negative allosteric modulators to reduce cue-induced reinstatement [16–18, 50]. Some evidence suggests that drug-induced increases in mGlu5 receptor availability, which predicted the degree of cue-induced reinstatement, is associated with disrupted negative outcome updating [51]. Taken together, this literature supports the use of mGlu5 receptor negative allosteric modulators to help people with AUD reduce alcohol craving and relapse.

A number of limitations and technical considerations are noted to aid interpretation of the presented results. First, given known brain atrophy associated with AUD [45], we compensated for possible atrophy influencing the PET data (typically causing underestimation of V_T when atrophy is present) by including partial volume correction (PVC). Analysis of the data without PVC did not reveal a significant main effect of AUD ($F_{(1,32)} = 2.77$), however, post-hoc analyses confirmed similar trends for higher non-PVC [^{18}F]FPEB V_T in AUD in the dlPFC, OFC, insula, and occipital cortex (see Supplementary Fig. 3). Although not a primary goal of this project, to assess group differences in gray matter volumes an exploratory voxelwise analysis was performed. Gray matter maps were smoothed with an 8 mm Gaussian kernel and compared with models including total intercranial volume as a covariate using statistical parametric mapping (SPM12; https://www.fil.ion.ucl.ac.uk/spm/software/spm12/). A two-sample *t*-test ($p < 0.001$, uncorrected) identified large clusters (>200 voxels) of less gray matter volume in people with AUD at early abstinence compared to healthy controls in occipital cortex (see Supplementary Fig. 4). There was no evidence for within-subject changes in gray matter volume from early to extended alcohol abstinence. Taken together, these observations increase confidence that the results were not overly biased by PVC effects. Second, variability in the timing of PET scans, relative to both the time of last drink and time of last lorazepam dose, may present a possible confound. Although our secondary analyses did not suggest any significant relationships of mGlu5 receptor availability with these variables, these factors may yet have influenced the results. Finally, the limited sample size does not allow a full exploration of potential interactive effects of AUD tobacco smoking together, which remains an important question for future research.

In summary, the presented study provides evidence for higher mGlu5 receptor availability in cortical brain regions in people with AUD at ~1 week of abstinence compared to control levels, which do not significantly change at 4 weeks of abstinence. These findings are consistent with a robust preclinical literature supporting mGlu5 receptor drugs as pharmacotherapies for AUD.

FUNDING AND DISCLOSURE

This work was funded by NIH grants K01AA024788, R01MH104459, P50AA012870, Yale Center for Clinical Investigation (NCATS UL1 TR001863), Dana Foundation, and State of Connecticut Support for the Clinical Neuroscience Research Unit. ATH, GAA, IE, JMA, NN, KL, JR, REC, and KPC declare no potential conflicts of interest. JHK reports having received consulting payments from AstraZeneca Pharmaceuticals, Biogen, Biomedisyn Corporation, Bionomics, Boehringer Ingelheim International, COMPASS Pathways, Concert Pharmaceuticals, Epiodyne, EpiVario, Heptares Therapeutics, Janssen Research & Development, Otsuka America Pharmaceutical, Perception Neuroscience Holdings, Spring Care, Sunovion Pharmaceuticals, Takeda Industries, and Taisho Pharmaceutical. He has served on advisory boards for Bioasis Technologies, Biohaven Pharmaceuticals, BioXcel Therapeutics, BlackThorn Therapeutics, Cadent Therapeutics, Cerevel Therapeutics, EpiVario, Eisai, Lohocla Research Corporation, Novartis Pharmaceuticals Corporation and PsychoGenics. He is a co-sponsor of a patent for the intranasal administration of ketamine for the treatment of depression and for the treatment of suicide risk that was licensed by Janssen Pharmaceuticals; has a patent related to the use of riluzole to treat anxiety disorders that was licensed by Biohaven Pharmaceuticals; has stock or stock options in Biohaven Pharmaceuticals, Blackthorn Therapeutics, Luc Therapeutics, Cadent Pharmaceuticals, Terran Biosciences, Spring Healthcare, and Sage Pharmaceuticals. He serves on the Board of Directors of Inheris Pharmaceuticals. He receives compensation for serving as editor of the journal Biological Psychiatry. SSOM reports being a consultant or an advisory board member of Alkermes, Indivior, Mitsubishi Tanabe, and Opiant; a NIDA Clinical Trials Network DSMB member with honorarium from the Emmes Corporation and nonfinancial support from Amygdala Neurosciences, Astra Zeneca and Novartis; and was a member of the American Society of Clinical Psychopharmacology's Alcohol

Clinical Trials Initiative (ACTIVE Group), which was supported by Alkermes, Amygdala Neurosciences, Arbor Pharmaceuticals, Ethypharm, Indivior, Lundbeck, Mitsubishi, and Otsuka. The authors declare no competing interests.

ACKNOWLEDGEMENTS

We are grateful to the staff at the Clinical Neuroscience Research Unit for their care of study participants and assistance with data collection. We thank the staff at the Yale PET center for their expertise and support of radiochemistry and imaging procedures. Elizabeth Guidone contributed excellent support in recruitment efforts. We thank Drs. Stephanie Groman, Adam Mecca, and Kelly Smart for insightful technical conversations.

AUTHOR CONTRIBUTIONS

This study was designed by ATH, REC, JHK, SSOM, and KPC. GAA was the study physician. Radiochemical production and quality control of [^{18}F]FPEB was carried out under the supervision of NN and YH. PET image acquisition was overseen by ATH, IE, REC, and KPC. Image analysis, statistical analysis, and initial drafting of the manuscript were performed by ATH. All authors provided editing contributions to this article.

ADDITIONAL INFORMATION

Supplementary Information accompanies this paper at (https://doi.org/10.1038/s41386-020-00856-9).

Publisher's note Springer Nature remains neutral with regard to jurisdictional claims in published maps and institutional affiliations.

REFERENCES

1. Cosgrove KP, McKay R, Esterlis I, Kloczynski T, Perkins E, Bois F, et al. Tobacco smoking interferes with GABAA receptor neuroadaptations during prolonged alcohol withdrawal. Proc Natl Acad Sci USA. 2014;111:18031–6.
2. Narendran R, Mason NS, Paris J, Himes ML, Douaihy AB, Frankle WG. Decreased prefrontal cortical dopamine transmission in alcoholism. Am J Psychiatry. 2014;171:881–8.
3. Weiland BJ, Sabbineni A, Calhoun VD, Welsh RC, Bryan AD, Jung RE, et al. Reduced left executive control network functional connectivity is associated with alcohol use disorders. Alcohol Clin Exp Res. 2014;38:2445–53.
4. Sullivan EV, Rosenbloom MJ, Lim KO, Pfefferbaum A. Longitudinal changes in cognition, gait, and balance in abstinent and relapsed alcoholic men: relationships to changes in brain structure. Neuropsychology. 2000;14:178.
5. Olive MF, Cleva RM, Kalivas PW, Malcolm RJ. Glutamatergic medications for the treatment of drug and behavioral addictions. Pharmacol Biochem Behav. 2012;100:801–10.
6. Nelson TE, Ur CL, Gruol DL. Chronic intermittent ethanol exposure enhances NMDA-receptor-mediated synaptic responses and NMDA receptor expression in hippocampal CA1 region. Brain Res. 2005;1048:69–79.
7. Umhau JC, Momenan R, Schwandt ML, Singley E, Lifshitz M, Doty L, et al. Effect of acamprosate on magnetic resonance spectroscopy measures of central glutamate in detoxified alcohol-dependent individuals: a randomized controlled experimental medicine study. Arch Gen Psychiatry. 2010;67:1069–77.
8. Kalivas P, Volkow N. New medications for drug addiction hiding in glutamatergic neuroplasticity. Mol Psychiatry. 2011;16:974–86.
9. Ango F, Prezeau L, Muller T, Tu JC, Xiao B, Worley PF, et al. Agonist-independent activation of metabotropic glutamate receptors by the intracellular protein Homer. Nature. 2001;411:962–5.
10. Mao L, Wang JQ. Glutamate cascade to cAMP response element-binding protein phosphorylation in cultured striatal neurons through calcium-coupled group I metabotropic glutamate receptors. Mol Pharmacol. 2002;62:473–84.
11. Tu JC, Xiao B, Naisbitt S, Yuan JP, Petralia RS, Brakeman P, et al. Coupling of mGluR/Homer and PSD-95 complexes by the Shank family of postsynaptic density proteins. Neuron. 1999;23:583–92.
12. Besheer J, Grondin JJ, Cannady R, Sharko AC, Faccidomo S, Hodge CW. Metabotropic glutamate receptor 5 activity in the nucleus accumbens is required for the maintenance of ethanol self-administration in a rat genetic model of high alcohol intake. Biol Psychiatry. 2010;67:812–22.
13. Cowen MS, Djouma E, Lawrence AJ. The metabotropic glutamate 5 receptor antagonist 3-[(2-methyl-1,3-thiazol-4-yl)ethynyl]-pyridine reduces ethanol self-administration in multiple strains of alcohol-preferring rats and regulates olfactory glutamatergic systems. J Pharmacol Exp Ther. 2005;315:590–600.
14. Gupta T, Syed YM, Revis AA, Miller SA, Martinez M, Cohn KA, et al. Acute effects of acamprosate and MPEP on ethanol Drinking-in-the-Dark in male C57BL/6J mice. Alcohol Clin Exp Res. 2008;32:1992–8.
15. Schroeder JP, Overstreet DH, Hodge CW. The mGluR5 antagonist MPEP decreases operant ethanol self-administration during maintenance and after repeated alcohol deprivations in alcohol-preferring (P) rats. Psychopharmacology. 2005;179:262–70.
16. Sinclair CM, Cleva RM, Hood LE, Olive MF, Gass JT. mGluR5 receptors in the basolateral amygdala and nucleus accumbens regulate cue-induced reinstatement of ethanol-seeking behavior. Pharmacol Biochem Behav. 2012;101:329–35.
17. Gass JT, Trantham-Davidson H, Kassab AS, Glen WB Jr, Olive MF, Chandler LJ. Enhancement of extinction learning attenuates ethanol-seeking behavior and alters plasticity in the prefrontal cortex. J Neurosci. 2014;34:7562–74.
18. Sidhpura N, Weiss F, Martin-Fardon R. Effects of the mGlu2/3 agonist LY379268 and the mGlu5 antagonist MTEP on ethanol seeking and reinforcement are differentially altered in rats with a history of ethanol dependence. Biol Psychiatry. 2010;67:804–11.
19. Schumann G, Johann M, Frank J, Preuss U, Dahmen N, Laucht M, et al. Systematic analysis of glutamatergic neurotransmission genes in alcohol dependence and adolescent risky drinking behavior. Arch Gen Psychiatry. 2008;65:826–38.
20. Haass-Koffler CL, Goodyear K, Long VM, Tran HH, Loche A, Cacciaglia R, et al. A Phase I randomized clinical trial testing the safety, tolerability and preliminary pharmacokinetics of the mGluR5 negative allosteric modulator GET 73 following single and repeated doses in healthy volunteers. Eur J Pharm Sci. 2017;109:78–85.
21. Haass-Koffler CL, Goodyear K, Loche A, Long VM, Lobina C, Tran HH, et al. Administration of the metabotropic glutamate receptor subtype 5 allosteric modulator GET 73 with alcohol: a translational study in rats and humans. J Psychopharmacol. 2018;32:163–73.
22. Kupila J, Karkkainen O, Laukkanen V, Tupala E, Tiihonen J, Storvik M. mGluR1/5 receptor densities in the brains of alcoholic subjects: a whole-hemisphere autoradiography study. Psychiatry Res. 2013;212:245–50.
23. Laukkanen V, Kärkkäinen O, Kautiainen H, Tiihonen J, Storvik M. Increased [^{3}H] quisqualic acid binding density in the dorsal striatum and anterior insula of alcoholics: a post-mortem whole-hemisphere autoradiography study. Psychiatry Res: Neuroimaging. 2019;287:63–69.
24. Akkus F, Mihov Y, Treyer V, Ametamey SM, Johayem A, Senn S, et al. Metabotropic glutamate receptor 5 binding in male patients with alcohol use disorder. Transl Psychiatry. 2018;8:17.
25. Leurquin-Sterk G, Ceccarini J, Crunelle CL, Bd Laat, Verbeek J, Deman S, et al. Lower limbic metabotropic glutamate receptor 5 availability in alcohol dependence. J Nucl Med. 2018;59:682–90.
26. Ceccarini J, Leurquin-Sterk G, Crunelle CL, Bd Laat, Bormans G, Peuskens H, et al. Recovery of decreased metabotropic glutamate receptor 5 availability in abstinent alcohol-dependent patients. J Nucl Med. 2019;61:256–62.
27. Akkus F, Ametamey SM, Treyer V, Burger C, Johayem A, Umbricht D, et al. Marked global reduction in mGluR5 receptor binding in smokers and ex-smokers determined by [(11)C]ABP688 positron emission tomography. Proc Natl Acad Sci USA. 2013;110:737–42.
28. Hulka LM, Treyer V, Scheidegger M, Preller KH, Vonmoos M, Baumgartner MR, et al. Smoking but not cocaine use is associated with lower cerebral metabotropic glutamate receptor 5 density in humans. Mol Psychiatry. 2014;19:625–32.
29. Wong DF, Waterhouse R, Kuwabara H, Kim J, Brasic JR, Chamroonrat W, et al. 18F-FPEB, a PET radiopharmaceutical for quantifying metabotropic glutamate 5 receptors: a first-in-human study of radiochemical safety, biokinetics, and radiation dosimetry. J Nucl Med. 2013;54:388–96.
30. Sullivan JT, Sykora K, Schneiderman J, Naranjo CA, Sellers EM. Assessment of alcohol withdrawal: the revised clinical institute withdrawal assessment for alcohol scale (CIWA-Ar). Br J Addiction. 1989;84:1353–7.
31. Sobell LC, Sobell MB. Timeline follow-back. Measuring alcohol consumption. Springer; 1992. pp. 41–72.
32. Lim K, Labaree D, Li S, Huang Y. Preparation of the metabotropic glutamate receptor 5 (mGluR5) PET tracer [(18)F]FPEB for human use: an automated radiosynthesis and a novel one-pot synthesis of its radiolabeling precursor. Appl Radiat isotopes: including data, Instrum methods use agriculture, Ind Med. 2014;94:349–54.
33. Sullivan JM, Lim K, Labaree D, Lin S-f, McCarthy TJ, Seibyl JP, et al. Kinetic analysis of the metabotropic glutamate subtype 5 tracer [18F]FPEB in bolus and bolus-plus-constant-infusion studies in humans. J Cereb Blood Flow Metab. 2013;33:532–41.
34. Park E, Sullivan JM, Planeta B, Gallezot JD, Lim K, Lin SF, et al. Test-retest reproducibility of the metabotropic glutamate receptor 5 ligand [(1)(8)F]FPEB with bolus plus constant infusion in humans. Eur J Nucl Med Mol Imaging. 2015;42:1530–41.
35. DeLorenzo C, Gallezot J-D, Gardus J, Yang J, Planeta B, Nabulsi N, et al. In vivo variation in same-day estimates of metabotropic glutamate receptor subtype 5

binding using [11C] ABP688 and [18F] FPEB. J Cereb Blood Flow Metab. 2017;37:2716–27.
36. Carson RE, Barker WC, Liow J-S, Johnson CA, editors. Design of a motion-compensation OSEM list-mode algorithm for resolution-recovery reconstruction for the HRRT. 2003 IEEE nuclear science symposium. Conference record (IEEE cat. no. 03CH37515). IEEE; 2003.
37. Müller-Gärtner HW, Links JM, Prince JL, Bryan RN, McVeigh E, Leal JP, et al. Measurement of radiotracer concentration in brain gray matter using positron emission tomography: MRI-based correction for partial volume effects. J Cereb Blood Flow Metab. 1992;12:571–83.
38. Tzourio-Mazoyer N, Landeau B, Papathanassiou D, Crivello F, Etard O, Delcroix N, et al. Automated anatomical labeling of activations in SPM using a macroscopic anatomical parcellation of the MNI MRI single-subject brain. NeuroImage. 2002;15:273–89.
39. Innis RB, Cunningham VJ, Delforge J, Fujita M, Gjedde A, Gunn RN, et al. Consensus nomenclature for in vivo imaging of reversibly binding radioligands. J Cereb Blood Flow Metab. 2007;27:1533–9.
40. Kågedal M, Cselényi Z, Nyberg S, Raboisson P, Ståhle L, Stenkrona P, et al. A positron emission tomography study in healthy volunteers to estimate mGluR5 receptor occupancy of AZD2066—estimating occupancy in the absence of a reference region. NeuroImage. 2013;82:160–9.
41. Hillmer AT, Carson RE. Quantification of PET infusion studies without true equilibrium: a tissue clearance correction. J Cereb Blood Flow Metab. 2020;40:860–74.
42. DuBois JM, Rousset OG, Rowley J, Porras-Betancourt M, Reader AJ, Labbe A, et al. Characterization of age/sex and the regional distribution of mGluR5 availability in the healthy human brain measured by high-resolution [11C]ABP688 PET. Eur J Nucl Med Mol Imaging. 2015;43:152–62.
43. Smart K, Cox SML, Scala SG, Tippler M, Jaworska N, Boivin M, et al. Sex differences in [11C]ABP688 binding: a positron emission tomography study of mGlu5 receptors. Eur J Nucl Med Mol Imaging. 2019;46:1179–83.
44. Holmes A, Spanagel R, Krystal JH. Glutamatergic targets for new alcohol medications. Psychopharmacology. 2013;229:539–54.
45. Pfefferbaum A, Sullivan E, Mathalon D, Shear P, Rosenbloom M, Lim K. Longitudinal changes in magnetic resonance imaging brain volumes in abstinent and relapsed alcoholics. Alcohol: Clin Exp Res. 1995;19:1177–91.
46. Nandi A, Valentine H, McCaul M, Wong D. Glutamatergic abnormalities in a rodent model of alcohol abuse. J Nucl Med. 2016;57:1866a.
47. Laat B, Weerasekera A, Leurquin-Sterk G, Gsell W, Bormans G, Himmelreich U, et al. Effects of alcohol exposure on the glutamatergic system: a combined longitudinal 18 F-FPEB and 1 H-MRS study in rats. Addict Biol. 2018;24:696–706.
48. Smart K, Scala S, El Mestikawy S, Benkelfat C, Leyton M. Cocaine Addiction and mGluR5: Recent Advances From Behavioral and Positron Emission Tomography Studies. In: The Neuroscience of Cocaine. Elsevier;Academic Press 2017. pp. 269–78.
49. Hasin DS, Grant BF. The National Epidemiologic Survey on Alcohol and Related Conditions (NESARC) waves 1 and 2: review and summary of findings. Soc Psychiatry Psychiatr Epidemiol. 2015;50:1609–40.
50. Bäckström P, Bachteler D, Koch S, Hyytiä P, Spanagel R. mGluR5 antagonist MPEP reduces ethanol-seeking and relapse behavior. Neuropsychopharmacology. 2004;29:921–8.
51. Groman SM, Liu H, Hillmer AT, Fowles K, Holden D, Esterlis I. et al. Distinct roles of dopamine D3 and mGlu5 receptors in addiction-relevant behaviors in the rat. Neuropsychopharmacology. 2019;44:M217